

Kinetic modeling of drug substance synthesis considering slug flow characteristics in a liquid-liquid reaction

Shunsei Yayabe^a, Junu Kim^a, Yusuke Hayashi^a, Kazuya Okamoto^b, Keisuke Shibukawa^b, Hayao Nakanishi^b, Hirokazu Sugiyama^{a*}

^a Department of Chemical System Engineering, The University of Tokyo, 7-3-1, Hongo, Bunkyo Ward, Tokyo, 113-8656, JAPAN

^b Technology Development Division, Shionogi Pharma Co., Ltd. Hyogo, 660-0813, JAPAN

* Corresponding Author: sugiyama@chemsys.t.u-tokyo.ac.jp.

ABSTRACT

This work presents a kinetic model of drug substance synthesis considering slug flow characteristics in Stevens oxidation. The developed model is also applied to determine the feasible range of the process parameters. Flow experiments were conducted to obtain kinetic data, varying the inner diameter, temperature, and residence time. A kinetic model was developed for the change in concentrations of the starting material, products, and catalysis. In the kinetic model, slug flow was considered by including a volumetric mass transfer coefficient during this flow. In the initial experiments, early-stage kinetic data were insufficient, conducting additional experiments at shorter residence times. Furthermore, the initial model could not reproduce the residual of the starting material, introducing the oxidant consumption that inhibits the starting material consumption and improving the initial model. The improved model could reproduce experimental results and demonstrated that, as the inner diameter increases, the efficiency of mass transfer in slug flow decreases with slowing down the reaction. Moreover, the improved model was considered applicable to different scales. The developed model was used to simulate the yields of the desired product, and the dimer, and the process mass intensity, thereby determining the feasible range. As a result, it was shown that when methanol and oxidant concentration was either too high or too low, operating conditions fell outside the feasible range. This kinetic model with flow characteristics will be useful for the process design of drug substance synthesis using liquid-liquid reactions.

Keywords: Modelling and Simulations, Modelling, Simulation, Process Design

INTRODUCTION

Recently, in the production of drug substances (or active pharmaceutical ingredients), flow synthesis has attracted attention as an effective method. Flow synthesis is increasingly being introduced due to its various advantages, such as high surface volume ratio and small system size compared to conventional batch synthesis [1,2]. One of the promising applications that leverages the advantages of flow synthesis is liquid-liquid reactions [3,4]. By performing these reactions in flow synthesis, the interfacial contact between immiscible liquids could be increased, which is expected to enhance process efficiency.

When two immiscible liquids enter together in a flow reactor, unique flow patterns, especially like slug flow,

are formed [5]. Slug flow is a phenomenon where the liquids flow in alternating enclosed segments, making a dynamic interface. Flow patterns like slug flow are determined by the liquid properties (e.g., viscosity and density) and the reactor specifications and have a significant impact on the mass transfer. Previous studies have investigated the effect of slug flow on mass transfer in liquid-liquid reactions using computational fluid dynamics [6,7] and explored flow pattern changes in solvents and reactor specifications and improvements in mass transfer [8,9]. These studies provide valuable insights into the influence of flow characteristics on reaction. However, there is a lack of modeling approaches that simultaneously account for flow characteristics and reaction kinetics. The absence of such models prevents understanding the interaction between flow characteristics and reaction

kinetics, potentially resulting in suboptimal process design and diminishing yields in practical application.

In this study, we developed a kinetic model of drug substance synthesis by incorporating slug flow characteristics in a liquid-liquid reaction, with the aim to determine a feasible range of the process parameters. The target reaction was Stevens oxidation, which is a novel liquid-liquid reaction of organic and aqueous phases, producing the ester via a shorter pathway than the conventional route [10]. In this reaction, a catalyst which moves between organic and aqueous phases was used, and slug flow formation was necessary to enhance mass transfer efficiency. A model can consider slug flow characteristics. In pharmaceutical industry, models are effective in reducing the number of experiments. By using models, it becomes possible to identify a feasible range of the process parameters that satisfies quality. Therefore, the developed model was utilized to define the feasible range.

MATERIALS AND METHODS

Target Reaction and Flow Experiments

Figure 1 shows the target Stevens oxidation and the flow experiment overview. In this reaction, (4-nitrophenyl) methanol (SM, starting material) undergoes a reaction with methanol (MeOH), and oxidant (NaOCl).

Tetrabutylammonium bromide (TBAB) is the catalyst which moves between the organic and aqueous phases. The ester methyl 4-nitrobenzoate (DP, desired product), the impurity 4-nitrobenzyl 4-nitrobenzoate (Dimer), 4-nitrobenzoic acid (CA, carboxylic acid), 4-nitrobenzaldehyde (Ald, aldehyde) are produced.

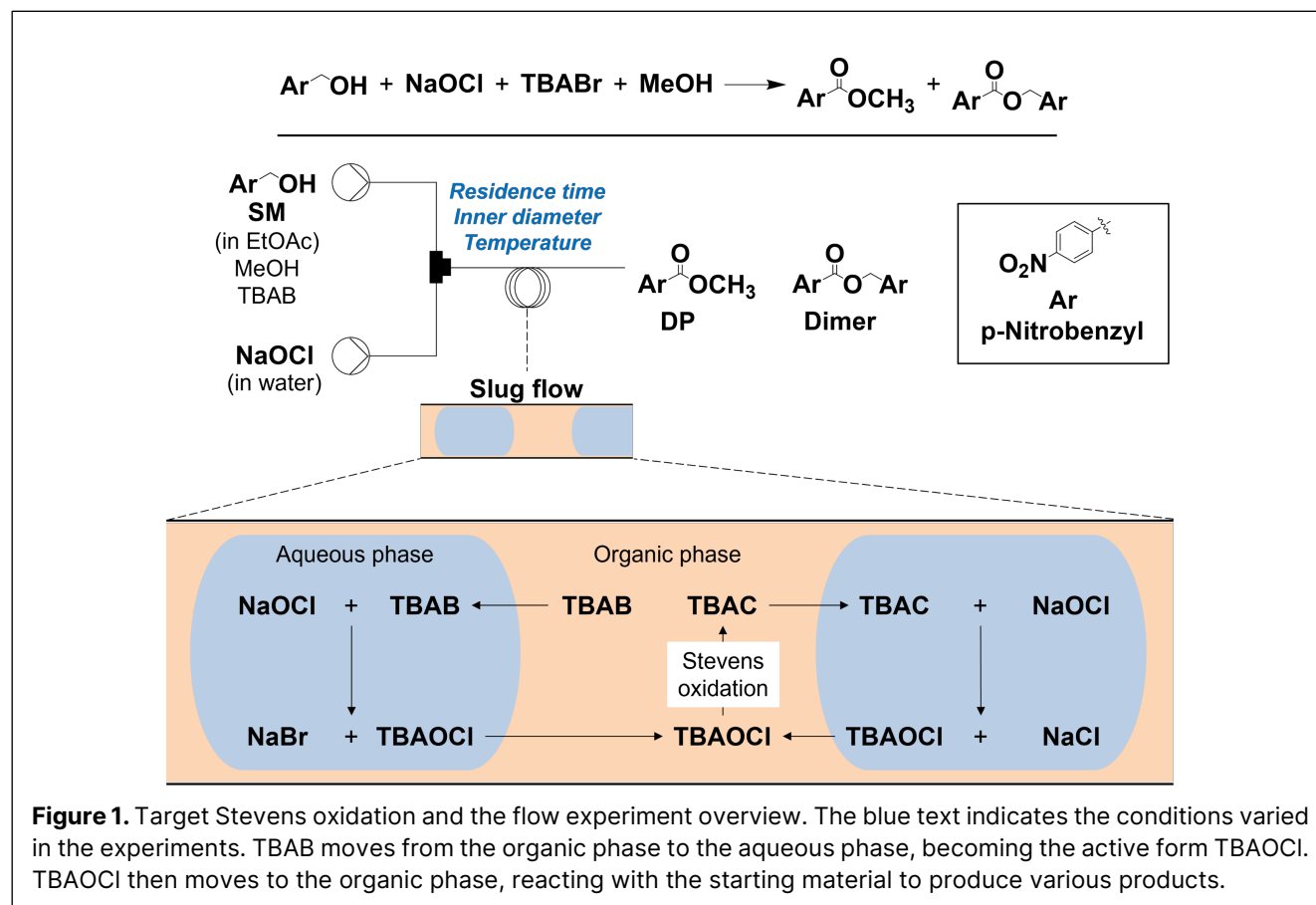
In the flow experiments, the inner diameter, temperature, and residence time were varied in different runs. Experimental conditions were adjusted to form slug flow to promote the catalyst's mass transfer. High-performance liquid chromatography (HPLC) was used to quantify the concentrations of SM, DP, Dimer, CA, and Ald in the samples.

Model Development

Figure 2 shows a calculation flow on the developed model. The inputs were defined as the equivalent concentration of MeOH, C_{MeOH} [equivalent], and the equivalent concentration of NaOCl, C_{NaOCl} [equivalent]. The outputs were defined as the yield of the desired product, y_{DP} [%], the yield of the dimer, y_{Dimer} [%], and the process mass intensity, PMI, which are evaluation indicators, respectively.

Kinetic model

The kinetic model was developed for the changes in concentration of SM, DP, Dimer, CA, Ald, and the catalyst.



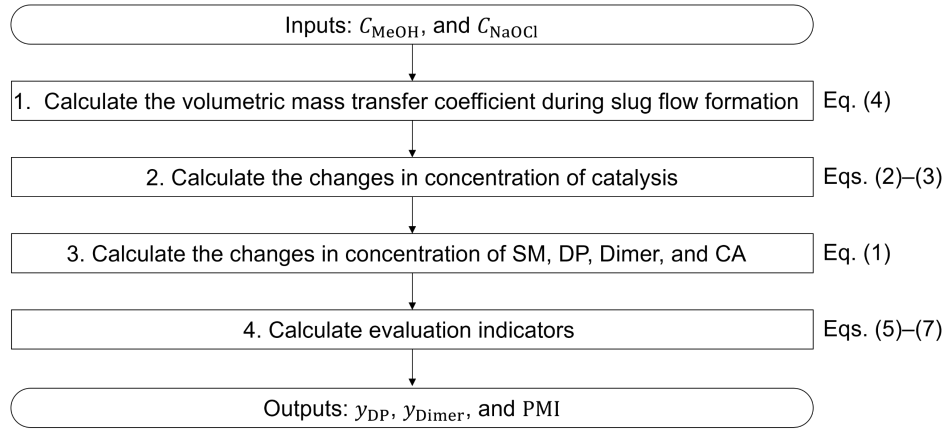


Figure 2. Calculation flow using the developed model. In the 1st step, the overall volumetric mass transfer coefficient during slug flow formation is calculated using Eq. (4). In the 2nd step, the changes in concentration of catalysis are calculated using Eqs. (2)–(3). In the 3rd step, the changes in concentration of SM and products are calculated using Eq. (1). Finally, in the 4th step, the evaluation indicators are calculated using Eqs.(5)–(7).

In the changes in the catalyst concentration model, slug flow was considered using the overall volumetric mass transfer coefficient during this flow formation. The changes in concentration were modelled as follows:

$$\frac{dC_i}{dt} = -r \quad (1)$$

$$\frac{dC_{j,org}}{dt} = -Ka_{org} \left(\frac{1}{m} C_{j,org} - C_{j,aqu} \right) - r \quad (2)$$

$$\frac{dC_{j,aqu}}{dt} = -Ka_{aqu} (m C_{j,aqu} - C_{j,org}) - r \quad (3)$$

Here, C_i [mol m⁻³] is the concentrations of i (SM, DP, Dimer, CA, and Ald), $C_{j,org}$ and $C_{j,aqu}$ [mol m⁻³] is the concentrations of j (TBAB, TBAOCl, and TBAC) in the organic and aqueous phases, r [mol m⁻³ s⁻¹] is the reaction rate, m [–] is the partition coefficient, Ka [s⁻¹] is the overall volumetric mass transfer coefficients in the organic and aqueous phases, and it was defined as follows [11]:

$$Ka_p \frac{L}{u_p} = \alpha Ca^\beta Re^\gamma \left(\frac{d}{L} \right)^\delta \left(\frac{L_p}{d} \right)^\varepsilon \quad (4)$$

Here, p is the phase (organic or aqueous), L [m] is the reactor length, u [m s⁻¹] is the flow velocity, Ca [–] is the mean capillary number of two phase, Re [–] is the mean Reynolds number of two phase, d [m] is the inner diameter, L_p [m] is the slug phase length in the organic and aqueous phases, and $\alpha, \beta, \gamma, \delta$, and ε are estimated parameters.

Evaluation model

To determine a feasible range of the process parameters, three evaluation indicators were determined in this study, namely, the yield of the desired product (y_{DP}) [%], the yield of the dimer (y_{Dimer}) [%], the process mass intensity (PMI) as follows:

$$y_{DP} = \frac{C_{DP}(L)}{C_{SM}(0)} \times 100 \quad (5)$$

$$y_{Dimer} = \frac{C_{Dimer}(L)}{C_{SM}(0)} \times 100 \quad (6)$$

$$PMI = \frac{mass_{SM}(0) + mass_{MeOH}(0) + mass_{NaOCl}(0) + mass_{TBAB}(0)}{mass_{DP}(L)} \quad (7)$$

Here, y_{DP} and y_{Dimer} [–] are the yields of DP and Dimer, PMI [–] is the process mass intensity, $C_{SM}(0)$ [mol m⁻³] is the initial concentration of SM at the inlet, $C_{DP}(L)$ and $C_{Dimer}(L)$ [mol m⁻³] are the concentrations of DP and Dimer at the outlet, $mass_i(0)$ [kg] is the mass of i (SM, MeOH, NaOCl, or TBAB) at the inlet, and $mass_{DP}(L)$ [kg] and $mass_{Dimer}(L)$ [kg] is the mass of DP and Dimer at the outlet.

Condition settings for feasible range

The feasible range was formulated as follows:

$$FR = \{(C_{MeOH}, C_{NaOCl}) : z(Y) = 1\} \quad (8)$$

Subject to

$$z(Y) = \begin{cases} 0 & (Y \notin S) \\ 1 & (Y \in S) \end{cases}$$

$$Y = f(C_{MeOH}, C_{NaOCl}, T, L, d, Q)$$

$$S = \{(y_{DP}, y_{Dimer}, PMI) : y_{DP} \geq 88, y_{Dimer} \leq 5, PMI \leq 15\}$$

$$C_{MeOH} \in \{10, 20, \dots, 70, 80\}$$

$$C_{NaOCl} \in \{3.0, 4.0, \dots, 7.0, 8.0\}$$

Here, FR is the feasible range, z takes the value of 1 if all evaluation indicators are satisfied and 0 if at least one evaluation indicator is not satisfied, S is a set of evaluation indicator constraints, and Y is the prediction results. In addition, T is temperature [K] and Q is the volume flow rate [mL m⁻¹].

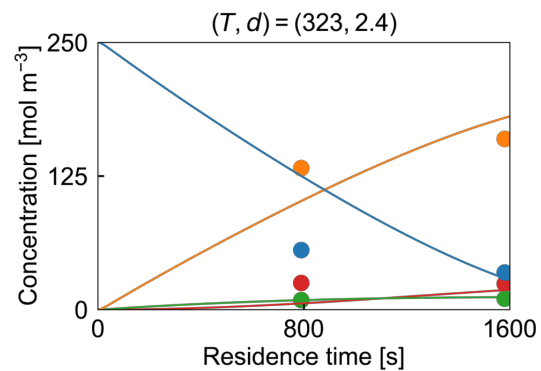
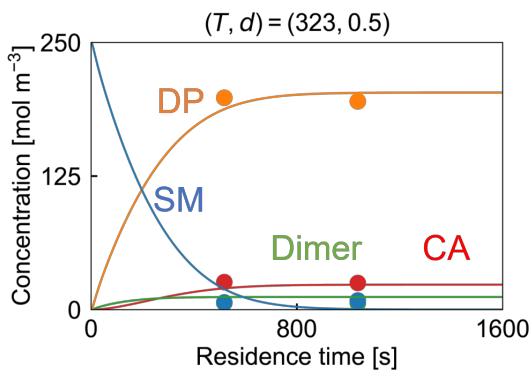
RESULTS AND DISCUSSION

Kinetic analysis

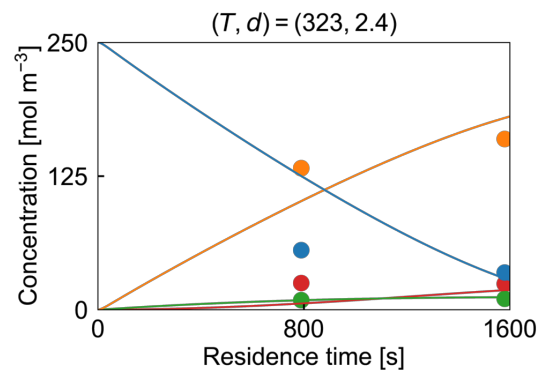
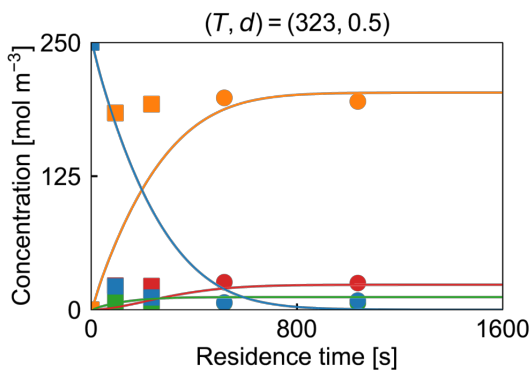
Fitting results of the initial model are shown in Figure 3(a). In the experimental conditions of $(T, d) = (323, 0.5)$, minimal changes in concentration were observed, and it was believed that the reaction had completed within the measurement residence time. Consequently, additional

experiments were performed at shorter residence times of $d = 0.5$ mm to obtain kinetic data during the early-stage reaction (Figure 3(b)). The initial model was unable to reproduce the results that included additional experiments. And then, residual SM was observed in the experiments, whereas the model predictions indicated its complete consumption. To address this discrepancy, the following hypothesis was proposed: SM undergoes with oxidant but competes with a mechanism in which oxidant is

(a) Fitting results of the initial model



(b) Additional experimental results and fitting results of the initial model



(c) Fitting results of the improved model

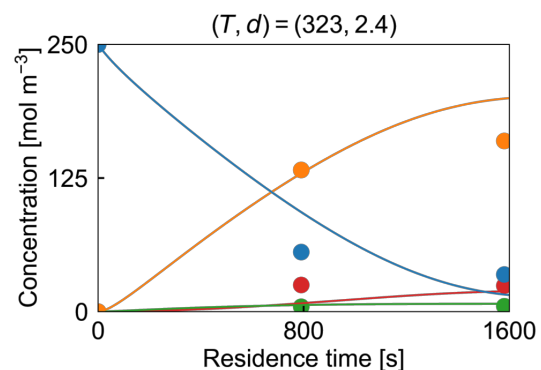
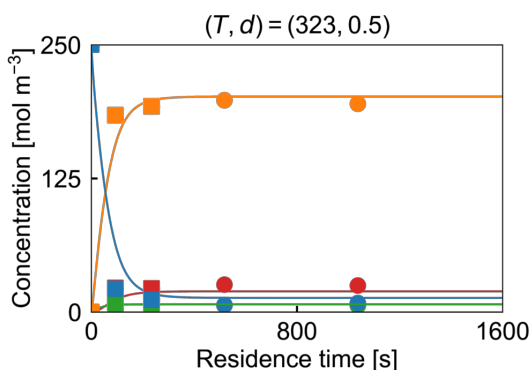


Figure 3. Fitting results, (a) of the initial model, (b) of the initial model only to the initial experimental results, and (b) of the improved model to all experimental results. Circles represent the initial experimental results, and squares represent the additional experimental results

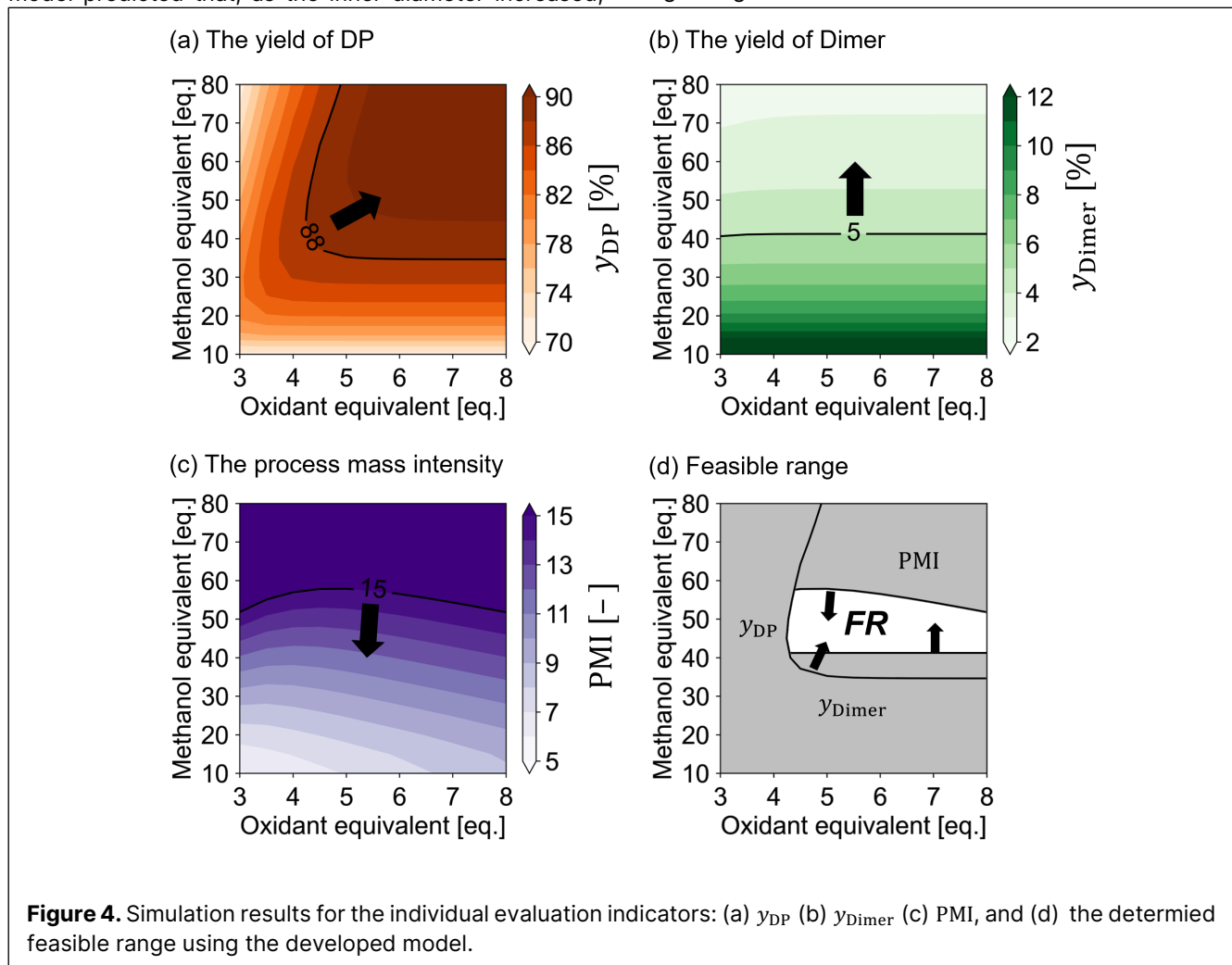
consumed through a different pathway, thereby limiting the consumption of SM. Based on the hypothesis, the methanol oxidation mechanism was added as an alternative pathway for the consumption of oxidant, and the model was improved accordingly. The improved model was used to conduct kinetic analysis again.

Fitting results of the improved model are shown in Figure 3(c). The average value of determination coefficients (R^2) of SM, DP, Dimer, and CA for all experimental conditions was 0.96, which means the model could reasonably reproduce experimental results. In this way, analyzing the discrepancies of the simulation results and the experimental results made it possible to select effective experimental conditions for the model development. The experimental results indicated that the reaction is slower under conditions with a larger inner diameter compared to those with a smaller inner diameter. This is believed to be due to the reduced mass transfer enhancement effect of slug flow as the inner diameter increases, resulting in a longer time required for catalyst movement. Indeed, it has been reported that larger inner diameters lead to slower mass transfer rates [12]. The model predicted that, as the inner diameter increased,

the efficiency of mass transfer in slug flow decreased with slowing the reaction, which is a similar trend of experiments. Therefore, we judged that the developed model could consider the slug flow characteristics and adopt to different scales and provide sufficient performance for determining the feasible range.

Feasible range determination and analysis

To determine a feasible range of the process parameters, the developed model was used to simulate the three evaluation indicators. The simulations were conducted within the range of the equivalent concentration of MeOH and NaOCl, as defined in Eq. (8). Figure 4 presents the results of (a) the yield of the desired product, (b) the yield of the dimer, (c) the PMI, and (d) feasible range. According to the simulation results, the high equivalent concentration of MeOH and NaOCl enhanced the yield of the desired product, and the high equivalent concentration of MeOH diminished the yield of the dimer. In contrast, as depicted in Figure 4(c), increasing the equivalent concentrations of MeOH and NaOCl caused to escalate the process mass intensity. High quality, meaning a large amount of DP and a small amount of Dimer,



was achieved with the high equivalent concentrations (C_{MeOH} and C_{NaOCl}). Conversely, low waste was attained at the low equivalent concentrations, indicating a trade-off in reagent quantity. Figure 4(d) shows the feasible range which satisfies the predefined constraints in Eq. (8) ($y_{\text{DP}} \geq 88, y_{\text{Dimer}} \leq 5, \text{PMI} \leq 15$), indicated by the white area. Within the range of the lower equivalent concentration of MeOH, the process did not meet the yield of the dimer. When the equivalent concentrations were too high, operating conditions fell outside the feasible range due to not satisfying the process mass intensity constraints. This feasible range could facilitate the identification of the process parameters that satisfied the constraints. Additionally, the feasible range could consider uncertainty and measurement noise by introducing stochastic approach such as Monte Carlo simulation.

CONCLUSIONS AND OUTLOOK

We presented the kinetic model of drug substance synthesis by incorporating slug flow characteristics and demonstrated the feasible range in Stevens oxidation. Flow experiments were conducted to obtain kinetic data, and a kinetic model considering flow characteristics was developed. For feasible range determination, the evaluation indicators developed, the yields and the process mass intensity. Utilizing the determined indicators, the feasible range was discussed, which could help in determining operating conditions. The kinetic model with slug flow characteristics would be useful for the process design of drug substance synthesis using liquid-liquid reactions. Future work includes conducting validation of the feasible range and presenting the scale-up strategy based on the simulation results using the developed model.

REFERENCES

1. Diab S, Raiyat M, and Gerogiorgis D. Flow synthesis kinetics for lomustine, an anti-cancer active pharmaceutical ingredient. *React Chem Eng* 6:1819–1828 (2021) <https://doi.org/10.1039/d1re00184a>
2. Silber K, Sagmeister P, Schiller C, Williams J, Hone C, and Kappe C. Accelerating reaction modeling using dynamic flow experiments, part 2: development of a digital twin. *React Chem Eng* 8:2849–2855 (2023) <https://doi.org/10.1039/d3re00244f>
3. Capaldo L, Wen Z, and Noël T. A field guide to flow chemistry for synthetic organic chemists. *Chem Sci* 16: 4230–4247 (2023) <https://doi.org/10.1039/d3sc00992k>
4. Plutschack M, Pieber B, Gilmore K, Seeberger P. The hitchhiker's guide to flow chemistry. *Chem Rev*

- 117: 11796–11893 (2017) <https://doi.org/10.1021/acs.chemrev.7b00183>
5. Ramji S, Rakesh A, Pushpavanam S. Modelling mass transfer in liquid-liquid slug flow in a microchannel. *Chem Eng J* 364:280–291 (2019) <https://doi.org/10.1016/j.cej.2019.01.075>
6. Cheng D, and Chen FE. Experimental and Numerical Studies of the Phase-Transfer-Catalyzed Wittig Reaction in Liquid-Liquid Slug-Flow Microchannels. *Ind Eng Chem Res* 59:4397–4410 (2020) <https://doi.org/10.1021/acs.iecr.0c00130>
7. Mittal A, Bhattacharyya S, Marino M, Chen TY, Desir P, Ierapetritou M, and Vlachos DG. Effect of Scale-Up on Mass Transfer and Flow Patterns in Liquid-Liquid Flows Using Experiments and Computations. *Ind Eng Chem Res* 62:15006–15017 (2023) <https://doi.org/10.1021/acs.iecr.3c02284>
8. Wei Y, Zhao S, Yu P, Yuan F, Li C, He W, Zhu N, Li Y, Ji D, and Guo K. Comparative studies of fluid mixing and heat transfer behaviors in a millimeter scale T-type mixer with triangular baffles. *Case Stud Therm Eng* 47:103076 (2023) <https://doi.org/10.1016/j.csite.2023.103076>
9. Yang N, Xiao Z, Liu F, Jiang J, Liu Z, Liu H, Yang X, and Wang R. Enhanced liquid-liquid mass transfer in a monolithic reactor with multi-jet-channel in the circumferential array. *Sep Purif Technol* 333: 125749 (2024). <https://doi.org/10.1016/j.seppur.2023.125749>
10. Wan L, Jiang M, Cheng D, Liu M, and Chen F. Continuous flow technology—a tool for safer oxidation chemistry. *React Chem Eng* 3: 490–550 (2022) <https://doi.org/10.1039/d1re00520k>
11. Kashid MN, Gupta A, Renken A, and Kiwi-Minsker L. Numbering-up and mass transfer studies of liquid-liquid two-phase microstructured reactors. *Chem Eng J* 158:233–240 (2010) <https://doi.org/10.1016/j.cej.2010.01.020>
12. Zhang Q, Liu H, Zhao S, Yao C, and Chen G. Hydrodynamics and mass transfer characteristics of liquid-liquid slug flow in microchannels: The effects of temperature, fluid properties and channel size. *Chem Eng J* 15: 794–805 (2019) <https://doi.org/10.1016/j.cej.2018.10.056>

© 2025 by the authors. Licensed to PSEcommunity.org and PSE Press. This is an open access article under the creative commons CC-BY-SA licensing terms. Credit must be given to creator and adaptations must be shared under the same terms. See <https://creativecommons.org/licenses/by-sa/4.0/>

